Hindawi
International Journal of Optics
Volume 2022, Article ID 2712863, 6 pages
https://doi.org/10.1155/2022/2712863

Research Article

The Linear Fitting Method for Model of PIN Array Receiver in Space Optical Communication

H. Qinggui

Information Construction and Service Center, Neijiang Normal University, Neijiang 641100, Sichuan, China

Correspondence should be addressed to H. Qinggui; hu646100178@126.com

Received 22 December 2021; Revised 4 March 2022; Accepted 7 March 2022; Published 22 March 2022

Academic Editor: Yuan-Fong Chou Chau

We have proposed PIN array as receiver in space optical communication and adopted the double diode model, the widely accepted solar energy output theory, to study its characteristics of output current and voltage. In order to make the calculation simplified, the linear fitting method is put forward. Later, we adopt both the traditional method Newton-Raphson and the new linear fitting method to calculate the values of both maximum power and the corresponding voltage of 3×3 PIN array. The comparison result shows the calculated values with two methods are good consistent. It validates the feasibility of the new linear fitting method. In the next step, the experiment has been carried out. The experimental result validates the reasonability of adopting the double diode model to study PIN array. At the same time, it validates the feasibility of the new linear fitting method again.

1. Introduction

The combination of free space optical communication and ordinary optical fiber communication is considered to be a hopeful method to solve "the Last Mile Issue of Communication." As to the combination, the coupling of space light to optical fiber is the key issue. In order to address this question, many scholars have conducted extensive research [1–7]. In 2013, Zhang et al. set up the space optical coupling alignment platform; they adopted both the position sensor and fast reflector to track the spatial light spot [1]. In 2014, Luo et al. used adaptive fiber couplers (AFC) to establish a closed loop control system to improve the coupling efficiency [2]. In 2014, Lei et al. adopted both the stepper motor and self-focusing lens to find the best coupling position in fiber array [3]. In reference [4], the authors present a new cladding design for high birefringence and low confinement loss photonic crystal fibers (PCFs) using a full-vector finite element method with anisotropic perfectly matched boundary layer. In reference [5], the authors propose a novel high-birefringence index-guiding photonic crystal fiber (PCF). This PCF is composed of a solid silica core and a cladding with two differently sized squeezed elliptical air-holes. In our previous works, we have proposed the conical fiber receiver to improve coupling efficiency and have studied its features from various perspectives [6–9]. Generally speaking, in these researches, the single optical fiber is used as the receiving device. The receiving area of the single optical fiber is too small; it brings difficulty for the coupling.

In recent years, some scholars have begun to apply PIN photodiodes in FSO communication systems. In [10], the authors design and demonstrate an integrated receiver for a visible light communication (VLC) system based on LED and an array of silicon PIN diode detectors. In [11], based on PIN photodiode receivers, the authors employ both asymmetric density evolution technique and an optimization scheme combined search algorithms to optimize low-density parity-check (LDPC) codes for FSO systems. In [12], with the cascaded preequalization circuit, and a differential outputs PIN receiver, the authors proposed a cascaded amplitude equalizer for high-speed visible light communications (VLC) system. In our previous work, we have proposed 3×3 PIN diode array to receive the spatial light, each PIN photodiode could independently receive the space laser and convert it into electrical signals [13].

The above literatures have studied PIN photodiode from various perspectives but failed to consider the effect of uneven illumination. In PIN diode array, due to the different

light intensities, different PIN diode produces different amount of photocurrent. In order to track the maximum output power, we should build mathematical models to analyze the characteristics of output current and voltage. But such research is relatively lacking. For the question of how to track the maximum power, there are many interesting studies in the field of solar energy technology. They discovered the single photovoltaic cell can be regarded as a photoelectric cell. Its current and voltage characteristics can be described with double diode model. Then, the double diode equation in photovoltaic model is used to describe the current and voltage characteristics of PIN diode. Later, Newton-Raphson method is adopted to resolve the resolution. In this work, we attempt to adopt this method to study PIN array receiver in space optical communication. This is our innovation. Considering that the calculation of Newton-Raphson method is too complicated, we adopt the linear fitting method to do the calculation work. This is our innovation as well. At the same time, the experiment is carried out whose results prove the proposed linear fitting method is reasonable.

2. The Equivalent Circuit Model

In the photovoltaic cell, P-N junction absorbs light energy and turns it into electrical energy. In order to prevent current backflow, the bypass diode is required in the circuit. Based on engineering practice and theoretical analysis, the single photovoltaic cell can be regarded as a photoelectric cell. Its current and voltage characteristics can be described with double diode model [14–16]. For single PIN diode, it is similarly true [17, 18]. We can use the double diode equation in photovoltaic model to describe the current and voltage characteristics of PIN diode, as shown in Figure 1. Normally, the value of R_{sh} is large, its impact on the open-circuit voltage and short-circuit current is little; we can ignore its influence. Then, the output current of single PIN diode I is given by [19, 20].

$$I = I_{ph} - I_d, \tag{1}$$

where I_{ph} is the photocurrent of single PIN diode; and I_d is the diode current; it is given by [19, 20]

$$I_d = I_o\left\{\exp\left[\frac{q}{kAT}\left(U + IR_S\right)\right] - 1\right\}, \tag{2}$$

where I_o is the reverse saturation current; it could be determined by the following equation [19, 20]:

$$I_o = I_{rr}\left(\frac{T}{T_r}\right)^3 \exp\left[\frac{qE_g}{Ak}\left(\frac{1}{T_r} - \frac{1}{T}\right)\right]. \tag{3}$$

In the above two equations (2) and (3), q is the electronic charge (1.6×10^{-19}C), k is the Boltzmann constant (it is 1.38×10^{-23} J/K); T is the temperature of single PIN diode, T_r is the temperature under standard test condition, I_{rr} is the reverse saturation current on the temperature T_r, R_s is the equivalent series resistance (usually, it is hundred milli ohms or dozen milli ohms [21, 22]), A is the ideal factor of the single PIN diode, and E_g is the band gap energy.

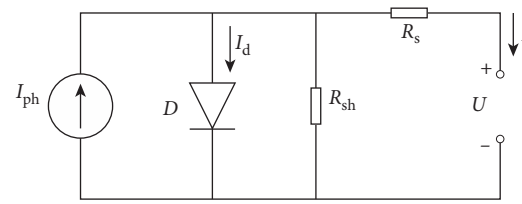

Figure 1: The equivalent circuit of a single PIN diode.

For the PIN diode array, as shown in Figure 2, to assume the number of PIN diodes in series is N_s, that in parallel is N_p, then the total number n is $N_s \times N_p$, we can gain the array's V-I characteristic equation [21, 22]:

$$I = N_p I_{ph} - N_P I_o\left\{\exp\left[\frac{q}{kAT}\left(\frac{U}{N_s} + \frac{IR_s}{N_p}\right)\right] - 1\right\}. \tag{4}$$

3. The Linear Fitting Method for PIN Diode Model

Formulas (1) and (4) are general mathematical models. However, they belong to exponential transcendental equations. Usually, we should adopt Newton-Raphson method to calculate it. But, this method needs large computation costs [23, 24]. Here, we put forward the new linear fitting method to simplify the calculation process.

With the MATLAB software, we can adopt the traditional method to figure out the relationship between the light intensity S_i and the voltage under maximum output power condition (we call it as maximum power voltage V_{mpp}). To assume the PIN array is 3×3, the ideal factor A is 1.2, and the band gap energy E_g is 1.12, the temperature unchanged (T is 25°C), then we can gain the relationship between V_{mpp} and S_i, as shown in the actual curve in Figure 3.

As shown in the actual curve in Figure 3, we can use the following linear equation to describe the relation between V_{mpp} and S_i [25, 26].

$$V_{mpp}{}' = k_1 \ln\left(\frac{S_i}{S_{ir}}\right) + b_1, \tag{5}$$

where $V_{mpp}{}'$ is the fitting maximum power voltage, and S_{ir} is the standard light intensity (100 mW/cm^2). This equation's meaning is that we can use this fitting equation to describe the relation between V_{mpp} and S_i, as the fitting curve shown in Figure 3.

To assume light intensity maintained unchanged, for example, it is 20 mW/cm^2. We use the traditional Newton-Raphson method to resolve the mathematical model formula from (1) to (4). Then, we can figure out the relationship between maximum power voltage V_{mpp} and temperature T, as shown in Figure 4. From those data points in the figure, we use equation (6) to describe the relation between the fitting maximum power voltage $V_{mpp}{}'$ and the maximum power voltage V_{mpp},

$$V_{mpp}{}' = V_{mpp} + k_T\left(25 - T\right), \tag{6}$$

where k_T is the temperature coefficient.

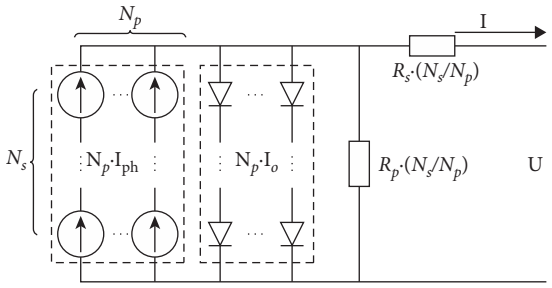

Figure 2: The equivalent circuit model of PIN array.

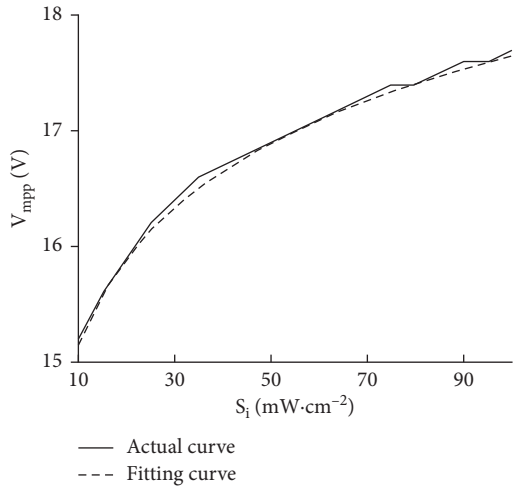

Figure 3: The actual curve and fitting curve between V_{mpp} and S_i.

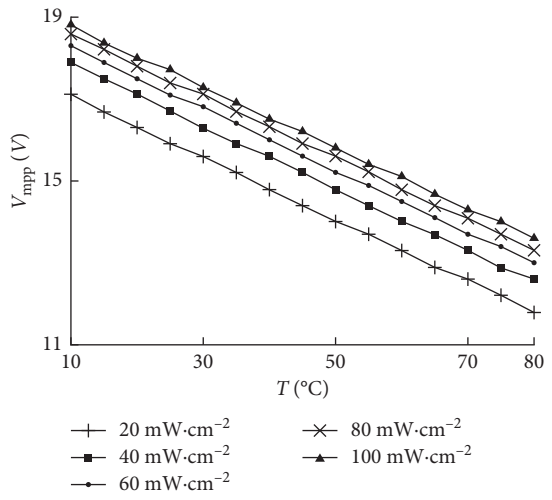

Figure 4: The relations between V_{mpp} and T under different S_i.

In the next step, when S_i are 40, 60, 80, and 100 mW/cm^2, we can repeat the above calculation process to gain the different fitting lines, as shown in Figure 4. We can see that, when S_i is different, the influence of temperature on the relations between $V_{mpp}{}'$ and V_{mpp} is different. Then, we use equation (7) to describe the relation between the temperature coefficient k_T and the light intensity S_i.

$$k_T = k_2 S_i + b_2. \tag{7}$$

Similarly, when S_i are 20, 40, 60, 80, and 100 mW/cm^2, we can gain the relation curves between the maximum output power P_{mpp} and V_{mpp}, as shown in Figure 5. From the figure, we can also discover that when S_i is maintained unchanged, we can use the following linear equation to describe the relation between P_{mpp} and V_{mpp}.

$$P_{mpp} = k_v V_{mpp} + b_v. \tag{8}$$

In the above equation, the coefficients k_v and b_v are related with S_i; we can look them as the functions of the light intensity S_i.

$$\begin{aligned} k_v &= k_3 S_i + b_3, \\ b_v &= k_4 S_i + b_4. \end{aligned} \tag{9}$$

From the above process, it can be seen that we can use the fitting linear equations to describe the relation between P_{mpp}, V_{mpp}, and S_i. The fitting linear equations can make the solving process simplified.

4. The Calculation Comparison between the Linear Fitting Method and Traditional Newton-Raphson Method

For the coefficients k_1 and b_1 in equation (5), we adopt the least-square method to compute their values [14–16]. The specific method is like the following steps. We select a lot of points on the actual curve in Figure 2, use S_{ii} to represent their abscissa values, use V_{mppi} to represent their ordinate values, and use n to represent the total number of discrete points. Then, the coefficients k_1 and b_1 are given by

$$\begin{aligned} k_1 &= \frac{\sum S_{ii} \sum V_{mppi} - n \sum S_{ir} V_{mppi}}{\left(\sum S_{ii}\right)^2 - n \sum S_{ii}^2}, \\ b_1 &= \frac{\sum \left(S_{ii} V_{mppi}\right) \sum S_{ii} - \sum V_{mppi} \sum S_{ii}^2}{\left(\sum S_{ii}\right)^2 - n \sum S_{ii}^2}. \end{aligned} \tag{10}$$

To assume the PIN array is 3 × 3, the ideal factor A is 1.2, and the band gap energy E_g is 1.12, with the above least-square method, we can work out the values of the coefficients k_1 and b_1, which are $k_1 = 1.082$ and $b_1 = 17.678$, and in this way, we can gain the values of other coefficients, like the following:

$$\begin{aligned} k_2 &= 0.0, \\ b_2 &= 0.076, \\ k_3 &= 0.039, \\ b_3 &= -0.541, \\ k_4 &= -0.044, \\ b_4 &= 8.540. \end{aligned} \tag{11}$$

In order to verify the effectiveness of this method, we make a comparison. Firstly, we adopt traditional Newton-Raphson method to calculate the values of both maximum

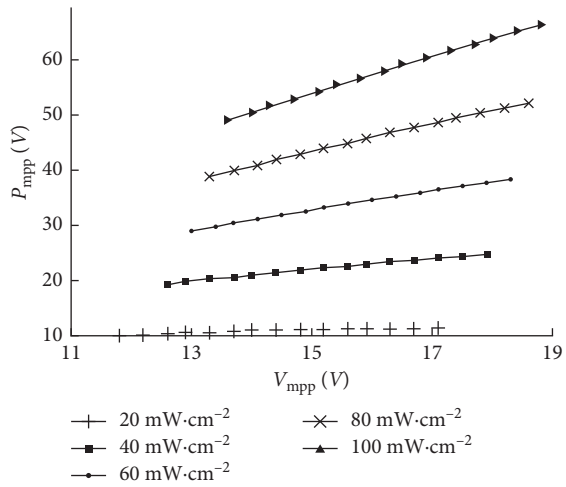

Figure 5: The relations between V_{mpp} and P_{mpp} under different S_i.

Table 1: Comparison between Newton-Raphson and proposed methods.

Temperature/°C	Light intensity/(mW/cm^2)	V_{mpp1}/V P_{mpp1}/W	V_{mpp2}/V P_{mpp2}/W	Error (δ)/%
25	100	17.75 61.81	17.68 62.51	0.39 1.13
35	80	16.32 45.76	16.30 46.05	0.12 0.6
50	60	14.87 32.37	14.61 32,65	1.7 0.86
60	40	13.25 20.10	13.01 20.31	1.81 1.04
70	20	11.82 10.03	11.79 10.46	0.25 4.28

power and the corresponding voltage, looking them as P_{mpp1} and V_{mpp1}. Then, we adopt new method to calculate the values of both maximum power and the corresponding voltage, looking them as P_{mpp2} and V_{mpp2}. Later, the relative error δ is defined as the following equations.

For V_{mpp},

$$\delta = \left| \frac{V_{mpp1} - V_{mpp2}}{V_{mpp1}} \right| \times 100\%. \quad (12)$$

For P_{mpp},

$$\delta = \left| \frac{P_{mpp1} - P_{mpp2}}{P_{mpp1}} \right| \times 100\%. \quad (13)$$

Finally, the result is shown in Table 1.

From Table 1, it can be seen that both V_{mpp1} and P_{mpp1} are coincident with V_{mpp2} and P_{mpp2}, respectively. It validates the feasibility of the new linear fitting method. Specifically, for the relative error δ, it changes from 0.25% to 4.28%; this value is very small. In other words, the matching degree is high.

In the view of the computational complexity, the traditional Newton-Raphson method needs to solve the transcendental equation. It includes the exponent arithmetic operations and needs multiple iterations. In a word, it needs much calculation cost. However, the linear fitting method does not need so much calculation. This method greatly simplifies the calculation process.

5. Experimental Test

In order to check the reasonability of the new linear method again, the author had a discussion with the technicians of Sichuan Coreway Optech Co., Ltd. At the same time, the test experiment is done.

In our previous work, as shown in Figure 6, we have produced 3×3 PIN array to do the experiment of space optical communication [13].

At this time, we also use this PIN array to do the test experiment. In this experiment, we use TES-1339 illuminometer to test the light intensity. TES-1339 illuminometer is produced in Taiwan; it is widely used in various industries and fields [4–7]. The experiment starts at 6:00 a.m. and ends at 2:00 p.m. At the same time, we adopt the new linear fitting method to calculate the theoretical data. In order to compare the experiment data with the theoretical data, we define the error rate in the following equation.

Error rate = (| measured data−theoretical data |/measured data) × 100%.

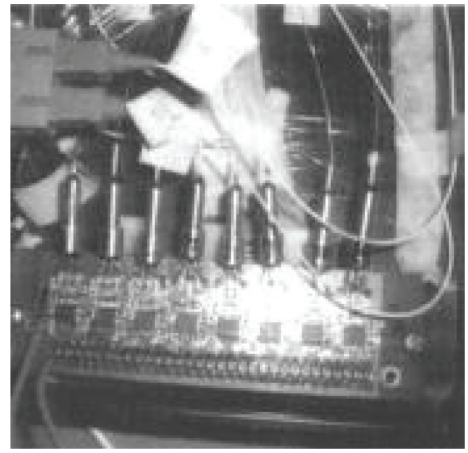

Figure 6: The appearance of the encapsulated PIN array.

Table 2: Comparison between experimental and proposed theoretical data.

Time	Temperature (°C)	Light intensity (W/cm^2)	Power (W)		Error rate (%)
			Measured data	Simulation data	
6:00	14	7	4.3	4.7	9.3
7:00	17	16	8.3	8.9	7.2
8:00	18.2	19	9.2	9.5	3.2
9:00	20.1	18	9.0	9.2	2.2
10:00	22	20	11	10.5	4.5
11:00	23	21	11.3	11.5	1.7
12:00	25	25	12.3	12.7	3.2
13:00	27	22	11.6	11.9	2.6
14:00	28	23	11.9	12.2	2.5

Finally, the measurement results and the error rate are shown in Table 2.

From Table 2, it can be seen that when the light intensity is low, the error rate is large. On the contrary, when the light intensity is high, the error rate is small. For example, when the light intensities are 7 W/cm^2 and 16 W/cm^2, the error rates are 9.3% and 7.2%, respectively. When the light intensities are 22 W/cm^2 and 23 W/cm^2, the error rates are 2.6% and 2.5%. This is because the losses of the instrument maintain unchanged. When the light intensity is lower, the fixed losses account for higher proportion. Then, the error is bigger. On the contrary, when the light intensity is higher, the fixed losses account for lower proportion. Then, the error is smaller.

From Table 2, it can be seen that the temperature also influences the error rate. When the temperature is low, the error rate is high. On the contrary, when the temperature is high, the error rate is low. For example, when the temperature is 14°C, the error rate is 9.3%. However, when the temperature is 28°C, the error rate is 2.5%. Maybe it is because of slightly underestimating the contribution of temperature in the double diode model. The new linear fitting method is deduced from the mathematical model. Thus, it produces the errors. In addition, the experimental data will be affected by the environmental parameters of last time. But this factor is not considered in the mathematical model. On the whole, the average error is about 4%; it shows the experimental result is in relatively good agreement with the numerical calculation result. The experiment proves the reasonability of the new linear fitting method again.

6. The Conclusion

The double diode model based on semiconductor diode theories have been widely used to extract the maximum power point of the solar PV array. In this paper, we use this model to study PIN array in space optical communication. Because the mathematical model contains transcendental equation, it makes the solving process complicated. In order to make the calculation simple, we put forward the new linear fitting method to do the calculation process. The comparison of calculation results has been conducted between the new and traditional methods. It shows the relative error δ changes from 0.25% to 4.28% in Table 2; this value is very small. In other words, matching degree is high. It validates the feasibility of the new linear fitting method. In addition, the test experiment has been carried out. The experimental data are compared with the theoretical data. By the comparison, we find it is reasonable to adopt the double diode model to study PIN array. At the same time, the experiment validates the feasibility of the new linear fitting method once more. This work shows we can use the linear fitting method to trace the maximum power of PIN array in FSO communication systems.

Data Availability

The data used to support the findings of this study are available from the author upon request.

Conflicts of Interest

The author declares no conflicts of interest.

Acknowledgments

This work was partially supported by the National Natural Science Foundation of China (Grant no. 61275080) and Solar Energy Integration Technology Popularization and Application Key Laboratory of Sichuan Province (2018TYNSYS-Z-01).

References

[1] R. Zhang, J. Wang, G. Zhao, and J. Lv, "Fiber-based free-space optical coherent receiver with vibration compensation mechanism," *Optics Express*, vol. 21, no. 15, p. 18434, 2013.

[2] W. Luo, C. Geng, and X. Li, "Simulation and experimental study of single -mode fiber coupling efficiency affected by atmospheric turbulence aberration," *Acta Optica Sinica*, vol. 34, no. 6, pp. 38–44, 2014, in Chinese.

[3] S. Lei, X. Ke, and J. Shao, "Experimental studyabout fiber array coupling and auto -alignment," *Laser Technology*, vol. 38, no. 2, pp. 191–195, 2014, in Chinese.

[4] K. Y. Yang, Y. F. Chau, Y. W. Huang, H. Y. Yeh, and D. Ping Tsai, "Design of high birefringence and low confinement loss photonic crystal fibers with five rings hexagonal and octagonal symmetry air-holes in fiber cladding," *Journal of Applied Physics*, vol. 109, no. 9, Article ID 093103, 2011.

[5] Y. Sun, Y. Chau, H. Yeh et al., "Highly birefringent index-guiding photonic crystal fiber with squeezed differently sized air-holes in cladding," *Japanese Journal of Applied Physics*, vol. 47, pp. 3755–3759, 2008.

[6] Q. Hu and Y. Mu, "Influence of vibration on the coupling efficiency in spatial receiver and its compensation method," *Optical Engineering*, vol. 57, no. 04, 2018.

[7] Q. Hu and C. Li, "The spatial light receiver and its coupling characteristics," *Optics Communications*, vol. 394, pp. 18–22, 2017.

[8] Q. Hu and C. Li, "The new tapered fiber connector and the test of its error rate and coupling characteristics," *International Journal of Optics*, vol. 2017, Article ID 2742709, 2017.

[9] Q. Hu and Y. Mu, "Analysis of the coupling efficiency of a tapered space receiver with a calculus mathematical model," *Laser Physics*, vol. 28, no. 3, Article ID 035104, 2018.

[10] J. H. Li, X. X. Huang, X. M. Ji, N. Chi, and J. Y. Shi, "An integrated PIN-array receiver for visible light communication," *Journal of Optics*, vol. 17, no. 10, Article ID 105805, 2015.

[11] J. Ao, J. Liang, C. Ma, G. Cao, C. Li, and Y. Shen, "Optimization of LDPC codes for PIN-based OOK FSO communication systems," *IEEE Photonics Technology Letters*, vol. 29, no. 9, pp. 727–730, 2017.

[12] X. Huang, Z. Wang, J. Shi, Y. Wang, and N. Chi, "16 Gbit/s phosphorescent white LED based VLC transmission using a cascaded pre-equalization circuit and a differential outputs PIN receiver," *Optics Express*, vol. 23, no. 17, pp. 22034–22042, 2015.

[13] H. U. Qinggui and M. U. Yining, "PIN photodiode array for free-space optical communication," *Photonic Network Communications*, vol. 36, no. 2, pp. 224–229, 2018.

[14] Panayiotis Nicos Kaloyerou, *The Method of Least Squares*, pp. 61–70, Basic Concepts of Data and Error Analysis, 2018.

[15] L. Csatóab, "A characterization of the logarithmic least squares method," *European Journal of Operational Research*, vol. 276, no. 1, pp. 212–216, 2019.

[16] L. L. Silva Ribeiro and A. Sri Ranga, "A modified least squares method: approximations on the unit circle and on (–1, 1)," *Journal of Computational and Applied Mathematics*, vol. 410, Article ID 114168, 2022.

[17] M. G. Villalva, J. R. Gazoli, and E. F. Ruppert, "Comprehensive approach to modeling and simulation of photovoltaic arrays," *IEEE Transations on Power Electronics*, vol. 25, no. 5, pp. 1198–1208, 2009.

[18] K. Prabu and D. S. Kumar, "MIMO free-space optical communication employing coherent BPOLSK modulation in atmospheric optical turbulence channel with pointing errors," *Optics Communications*, vol. 343, pp. 188–194, 2015.

[19] P. Kaur, V. K. Jain, and S. Kar, "Performance analysis of free space optical links using multi-input multi-output and aperture averaging in presence of turbulence and various weather conditions," *IET Communications*, vol. 9, no. 8, pp. 1104–1109, 2015.

[20] Y. Wu, *Application Research of Adaptive Optics Technique in Atmospheric Optical Communications*, University of Chinese Academy of Sciences, Beijing, China, 2013, in Chinses.

[21] T. Zheng-rong, W. Han, and Y. Cao, "Fiber sensor for simultaneous measurement of temperature and refraction index based on multi mode fiber core-offset," *Acta Optica Sinica*, vol. 34, no. 1, Article ID 0106004, 2014, in Chinses.

[22] G. L. Yin, S. Q. Lou, and H. Zou, "Refractive index sensor with asymmetrical fiber mach-zehnder interferometer based on concatenating single-mode abrupt taper and core-offset section," *Optics & Laser Technology*, vol. 45, pp. 284–300, 2013.

[23] K. Xizheng and Liu Mei, "Diversity reception technology over atmospheric turbulence channels in wireless optical communication," *Acta Optica Sinica*, vol. 35, no. 1, Article ID 0106005, 2015, in Chinses.

[24] F. Fontana and E. Bozzo, "Newton-raphson solution of nonlinear delay-free loop filter networks," *IEEE/ACM Transactions on Audio, Speech, and Language Processing*, vol. 27, no. 10, pp. 1590–1600, 2019.

[25] S. Kakita and Y. Okamoto, "Enhancement of convergence characteristics of newton-raphson method with line search for nonlinear eddy current analysis based on time-periodic FEM," *COMPEL—The International Journal for Computation and Mathematics in Electrical and Electronic Engineering*, vol. 38, no. 5, pp. 1627–1640, 2019.

[26] K. Prabu, D. S. Kumar, and R. Malekian, "BER analysis of BPSK-SIM-based SISO and MIMO FSO systems in strong turbulence with pointing errors," *Optik*, vol. 125, no. 21, pp. 6413–6417, 2014.